Science of Advanced Materials
Vol. 9, pp. 1683–1692, 2017
www.aspbs.com/sam

Toughening Poly(lactic acid) by Melt Blending with Poly(ether-*block*-amide) Copolymer

Jianchen Cai[1,*], Jinyun Jiang[1], Zhaozhong Zhou[1], Yun Ding[2], Yang Zhang[2], Fei Wang[2], Cui Han[3], Jiang Guo[4], Qian Shao[3], Huayun Du[4], Ahmad Umar[5,*], and Zhanhu Guo[4,*]

[1]*College of Mechanical Engineering, Quzhou University, Zhejiang, 324000, China*
[2]*College of Mechanical and Electrical Engineering, Beijing University of Chemical Technology, Beijing, 100029, China*
[3]*College of Chemical and Environmental Engineering, Shandong University of Science and Technology, Qingdao 266590, P. R. China*
[4]*Integrated Composites Laboratory (ICL), Department of Chemical and Biomolecular Engineering, University of Tennessee, Knoxville, TN 37996, USA*
[5]*Department of Chemistry, Faculty of Sciences and Arts, Promising Centre for Sensors and Electronic Devices (PCSED), Najran University, P.O. Box 1988, Najran, 11001, Saudi Arabia*

ABSTRACT

Melt blending with poly(ether-*b*-amide) copolymer (PEBA) was found to significantly enhance the toughness of poly(lactic acid) (PLA). The miscibility, morphology, thermal behavior, mechanical properties and rheological behavior of the blends were investigated. DMA and DSC analysis revealed that the PLA/PEBA blends were immiscible. A clear, phase-separated morphology was observed from SEM results. The addition of PEBA enhanced the cold crystallization of the PLA in the blends and accelerated the crystallization rate due to the interfacial function between PLA and PEBA phases. Significant enhancement of the toughness of PLA was achieved by the incorporation of PEBA copolymer. The optimum impact modification of the PLA was obtained by blending with 20 wt% PEBA, with an elongation at break of 300% as compared to 5% for pure PLA. The impact strength was ten times higher than that of the pure PLA. SEM results showed that the interfacial cavitation followed by a massive shear yielding of the matrix contributed to the increased toughening effect in the blends. The rheological measurement revealed an interaction between PLA and PEBA in the melt state.

KEYWORDS: Mechanical Properties, Toughness, Blending.

ARTICLE

1. INTRODUCTION

Over the past decade, increasing research interest has been grown in the biodegradable polymers prepared with renewable sources aiming to alleviate solid waste disposal issues and to reduce the usage of petroleum-based materials especially polymers.[1–3] Among these polymers, poly(lactic acid) (PLA) is one aliphatic polyester manufactured completely from renewable materials, and has drawn increasing attention and wide studies. Being degradable naturally and compatible with other biomaterials, improved mechanical properties and easy reshaping,[4] PLA has been widely studied for use in biomedical applications such as surgical suture, and drug delivery system; and in electronic devices. Recently, owing to its biomass origin, good performance and availability in the market at a reasonable price, PLA has been considered as a promising and ideal alternative to petroleum-based plastics in commercial applications, such as packaging, fiber materials.[4–7] However, PLA has only enjoyed limited success in replacing petroleum-based plastics in commodity applications today. It exhibits brittleness and its fracture strain is only about 5% in the tensile test, which results in poor impact and tear resistance. The inherent brittleness of PLA has been the major deficiency that hinders its large-scale applications in both commodity and biomedical areas.[6, 8–22] Accordingly, the development of PLA-based materials with high toughness has attracted wide attention in recent years.

Blending with other proper polymer has been justified as a promising way to improve the mechanical properties of PLA. Up to now, PLA has been melt processed with many flexible polymers to improve its toughness and flexibility.[8–17] Some interesting and noteworthy results have been reported, however, most of the blends needed compatibilizers to improve their compatibility to realize the desired mechanical properties.[17] Rubber toughening mechanisms developed on conventional thermoplastics have also been successfully applied

*Authors to whom correspondence should be addressed.
Emails: cai198666@126.com, umahmad@nu.edu.sa, zguo10@utk.edu
Received: 8 March 2017
Accepted: 3 May 2017

to biopolymers.[18] Blending with suitable elastomeric materials provides an effective method to improve the toughness of PLA.[13, 19–23] Poly(ether-*block*-amide) copolymer (PEBA) is a kind of important commercial thermoplastic elastomers with unique physical and processing properties. It is a segmented block copolymer consisting of an aliphatic polyamide as the hard block, a polyether as the soft block and a di-acid serving as the joint between the two blocks. PEBA offers a wide range of excellent performances and has been used in many fields such as antistatic sheets or belts, and packaging.[24, 25] More interestingly, PEBA has a good biocompatibility and finds wide uses in a variety of medical applications such as short-term implantation in humans and virus-proof surgical sheeting. Recently, it is announced by Arkema Company that this type polymer can be made from renewable materials including castor oil, which could reduce fossil-based material consumption by 29% and CO_2 equivalent emissions by 32%.[24] As a result, PEBA is an ideal blending constituent for PLA to prepare new environmentally benign material for uses in both biomedical and commodity applications. Meanwhile, PEBA has a high impact resistance even at temperature as low as −40 °C since the polyether-rich phase has a much lower glass transition temperature, and thus PEBA can be used as an impact modifier for the brittle thermoplastic polymer.[24, 25] Consequently, it is quite reasonable to expect that the introduction of PEBA into PLA may effectively enhance the flexibility and toughness of PLA. To our knowledge, the study of PLA/PEBA blends has not been reported so far.

In the present work, the blending PLA with a kind of PEBA was reported to improve the flexibility and toughness of PLA. The miscibility and morphology of the blend were studied. The effects of the presence of PEBA on the thermal behaviors, mechanical properties and rheological properties of the PLA in the blends were also thoroughly investigated.

2. MATERIALS AND METHODS

2.1. Materials

The Nature works PLA 4032D (weight-average molecular weight ($\bar{M}_w$): 207 kDa, polydispersity index: 1.74 (GPC analysis) was obtained from Nature Works LLC, USA. The PEBA was provided by Elf Atochem Inc., having a trade name of Pebax 2533, which comprises of hard poly(lauryl lactam) (PA 12) segment (12 wt%), soft poly(tetramethylene ether) glycol (PTMO, 84 wt%) segment, and adipic acid as the linkage (3.6 wt%). The weight percentages of the segment and linkage were determined from ^{1}H NMR spectra.[25]

2.2. Preparation of the Blends

Prior to blending, all the materials were dried overnight under vacuum, PLA at 60 °C and the PEBA at 80 °C, respectively. Blends of PLA/PEBA of varying compositions were prepared on the Haake Batch Intensive Mixer (Haake Rheomix 600, Germany). 50 mL blends was batch processed at 180 °C and a screw speed of 60 rpm for 8-min mixing, until the viscosity had reached a nearly constant value. Pure PLA was also processed following the same procedures used for the blends for comparison.

2.3. Characterizations

Dynamic mechanical analysis (DMA) was carried out with a Diamond DMA dynamic mechanical analyzer (PerkinElmer, American) in a tensile mode. The specimens with dimensions of $30 \times 10 \times 1$ mm^3 were used. The heating temperature was controlled from −100 to 140 °C, the heating rate was 3 °C/min, and the frequency was one Hz.

The morphology of the blends was observed by a scanning electron microscope (SEM, XL30 ESEM FEG, FEI Co.). The samples were prepared by breaking after processed in liquid nitrogen. Then the specimen was mounted on an aluminum stub using a conductive paint and finally sputtered with gold prior to fractographic examination. The different zones of the specimens after tensile tests and fracture surfaces obtained from notched Izod impact test were also characterized by SEM.

The differential scanning calorimetry (DSC) measurements were carried out on a TA Q100 DSC instrument under N_2 atmosphere. The samples were heated to 190 °C at a heating rate of 20 °C/min, maintained at 190 °C for 5 min before cooling down to −100 °C at a rate of 80 and 2 °C/min. The second heating scan was from −100 to 190 °C at a heating rate of 10 °C/min, from which the glass transition temperature (T_g), cold crystallization temperature (T_c') and melting temperature (T_m) were determined.

Wide angle X-ray diffraction analysis (WAXD) tests were done on a Rigaku D/max 2500 V PC X-ray diffractometer. The measurements were operated at 40 kV and 20 mA from 2°–40° at a 2θ scan rate of 4°/min.

Tensile properties were tested at room temperature with an Instron 1121 testing machine (Canton, MA) according to GB/T1040.3-2006 (China). The specimens were prepared by compression molding into sheets with a thickness of one mm, then being cut into a dumbbell shape with gauge dimensions of 20 mm × 4 mm × 1 mm. A crosshead rate of 10 mm/min was used. The data reported were the mean and standard deviation from five determinations.

The notched Izod impact strength was tested with a CEAST impact machine according to GB1843-93 (China).

The rheological measurements were carried out on a PHYSICA MCR 300 instrument (Stuttgart, Germany). The frequency sweep was carried out under nitrogen at 180 °C using 25 mm geometry with the sample gap being set as 0.6 mm. An initial strain sweep was tested to select the linear viscoelastic region of the materials. The strain was fixed at 5% and the angular frequency range was from 0.05 to 100 rad/s. The samples were pressed into 1 mm thick at about 190 °C. The data was obtained by using the MCR300 software.

3. RESULTS AND DISCUSSION

3.1. Miscibility of PLA/PEBA Blends

DMA was firstly employed to assess the miscibility of the polymer blends and the results, Figures 1(a) and (b). The observed Tanδ peak at about 63 °C, Figure 1(a), corresponds to its glass transition of the neat PLA. For pure PEBA, an intense Tanδ peak was observed at about −70 °C corresponding to the glass transition of PTMO segments in PEBA copolymer.[25] At the upside of this Tanδ peak, a minor shoulder was observed, and was assigned to the partial cold crystallization and melting behavior of the PTMO phase. No clear glass transition of PA12 phase was observed because the PA12 segments were shorter and possibly further mixed with some of the PTMO material, giving rise to a broadening and a downward shift in its T_g.[25] As for the blends, the Tanδ curves mainly exhibited two distinct Tanδ peaks, corresponding to the glass transition of the initial products in the blends. It was noticed that the T_g values of both components in the blends are almost independent of the blend composition. This indicates that these two components in the blend were immiscible. Figure 1(b) shows the storage modulus curves of the samples. In consistence with the Tanδ curve, no obvious change of the transition temperature of PLA can be observed for the blends due to the immiscibility of the two components. The E' of PLA/PEBA blends decreased with increasing the PEBA content in the blends at room temperature. Moreover, the temperature, at which the storage modulus started to increase, arising from the cold crystallization of PLA, shifted to a lower temperature compared with that of the neat PLA with the addition of PEBA. This phenomenon strongly suggested that the incorporation of PEBA elastomer enhanced the cold-crystallization ability of PLA and therefore decreased the cold-crystallization temperature of PLA in the blend.

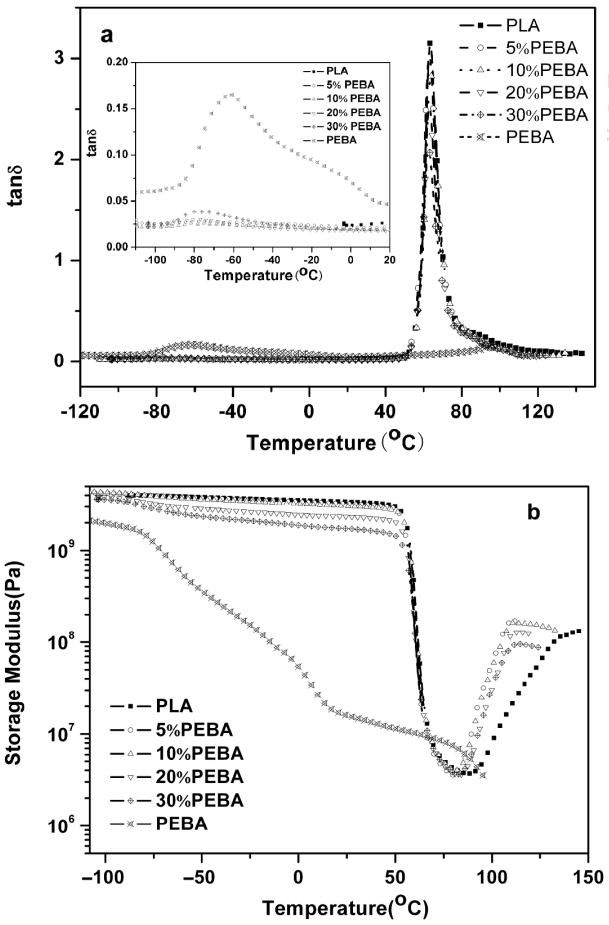

Fig. 1. DMA graphs of PLA blended with PEBA elastomer at various concentrations: (a) Tanδ versus temperature; (b) storage modulus versus temperature.

Figure 2 presents the SEM micrographs of PLA/PEBA blends. The PEBA phase domains are preferentially dispersed as spheres in the continuous PLA matrix with smooth and distinct interfaces. The approximate diameters of the dispersed PEBA phases are 0.3–1.5 μm with 5–20 wt% PEBA. With further increasing the content of PEBA, there was a corresponding increase in the PEBA particles size due to the coalescence. It is well known that the interfacial adhesion of blend was closely related to its miscibility. The clear, phase separation further testified that the two components have a poor miscibility.

3.2. Thermal and Crystallization Behaviors of PLA/PEBA Blends

Both PLA and PEBA are semi-crystalline polymers. Accordingly, it is important to study the influence of the existing PEBA on the crystallization of PLA. To study the presence of the PEBA on the cold crystallization of PLA, the samples were first quenched from the crystal free melt at a cooling rate of 80 °C/min by DSC. Figure 3 shows the cooling DSC thermograms at a cooling rate of 80 °C/min for neat polymer and its blends after melted at 190 °C for 5 min. During the cooling scan, no exothermic peak corresponding to the crystallization of the PLA component was observed in all the samples, indicating that the PLA was primarily amorphous when being cooled from melt at 80 °C/min. However, pure PEBA was still able to crystallize at this cooling rate, and two exothermic peaks corresponding to the crystallization of the PA12 segments and the PTMO segments of PEBA were observed. Figure 4 shows the second heating thermal scans. As for the neat PEBA, two separate melting peaks were observed, and were attributed to the melting of the two blocks.[25] The endothermic peak at around 10 °C was attributed to the melting behavior of PTMO crystal in PEBA copolymer. The melting behavior of PA12 crystal occurred at about 135 °C and a minor endothermic peak could be observed. Neat PLA exhibits a specific heat increment at about 61 °C ascribed to the glass-rubber transition of PLA. At higher temperature, an exothermal peak at 134 °C corresponding to the cold crystallization of PLA was observed. The melting of these crystallized domains occurred at 167 °C. The thermal behaviors of

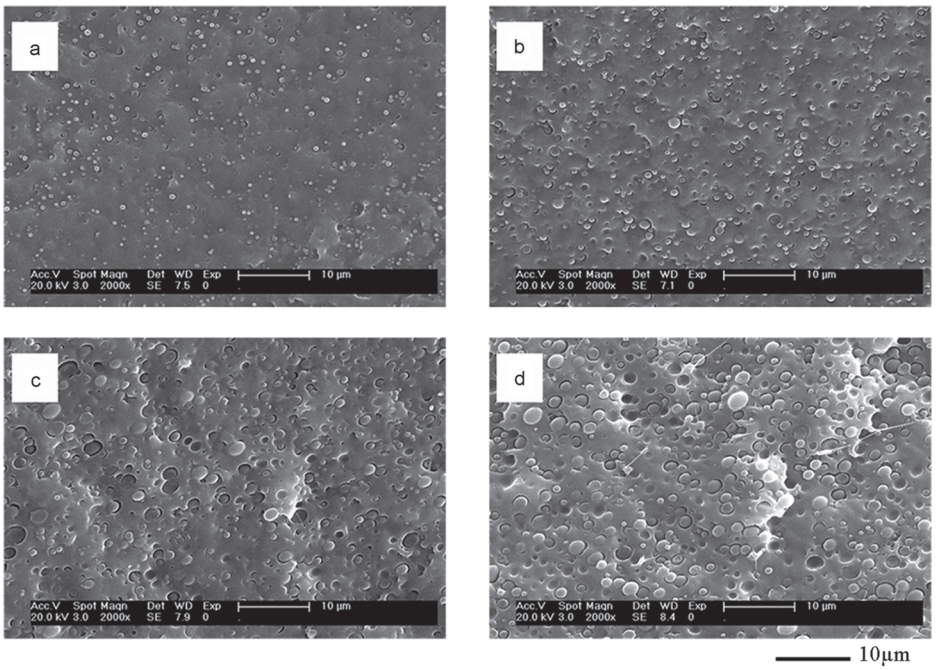

Fig. 2. SEM images of cryofractured surface of PLA/PEBA blend with a PLA/PEBA weight compositions of (a) 5 , (b) 10 , (c) 20 , and (d) 30 wt% PEBA.

the blends mainly showed the thermal transition of the PLA and the melting of the PTMO segment in the PEBA copolymer, while the melting of the PA12 crystal could not be clearly observed because the small concentration of PA12 segment in the blend and overlapped with the transition of PLA. As shown in Figure 4, in consistence with the DMA and SEM results, no obvious change of T_g and T_m of components was observed. This suggests that the two components were completely immiscible. Interestingly, the melting peak of PLA showed a transition from single peak to two separate peaks. Generally, multiple melting peaks of semi-crystalline polymers are attributed to two main reasons: melt-recrystallization and dual crystal structures. To further reveal the fact, WAXD patterns were determined for the samples subjected to the same thermal treatment as DSC. Figure 5 shows the WAXD patterns of PLA and the PLA/PEBA blends. As shown in Figure 5, the characteristic reflection peaks of α crystal PLA kept almost the same position regardless of the composition variation, indicating that the PLA unit cell never changed. Therefore, the bimodal melting peaks of the blends must be resulted from the melt-recrystallization. During the slow DSC scans, the less perfect crystals got enough time to melt and reorganize into crystals with higher structure perfection and remelt at higher temperature. Similar phenomena were also reported in other PLA blends.[14, 21–23]

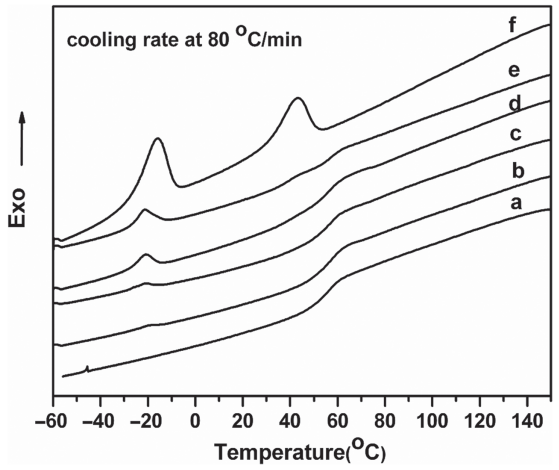

Fig. 3. The cooling DSC thermograms at a cooling rate of 80 °C/min for neat polymer and its blends after melted at 190 °C for 5 min.

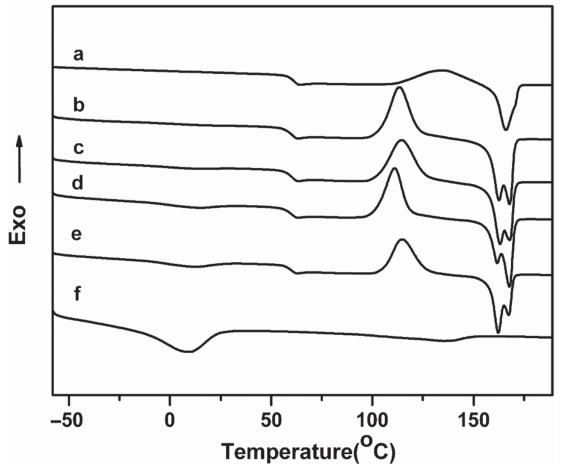

Fig. 4. The second heating DSC thermograms for PLA, PEBA and the blends.

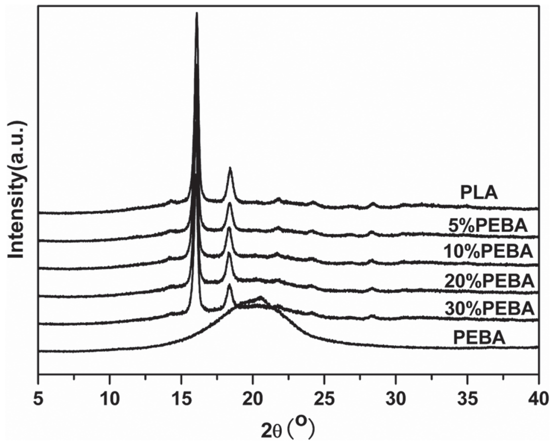

Fig. 5. The WAXD patterns of PLA and the PLA/PEBA blends.

However, the cold-crystallization exothermic peak of the blends was dramatically different from neat PLA. A tiny broad exothermic peak at 134 °C was observed for neat PLA, this indicated that PLA has a rather low cold crystallization capability. Compared with the neat PLA, the cold crystallization temperature (T_{cc}) of PLA in the blends was evidently found to shift towards a lower temperature region, and the width of exothermic peaks became narrower than that of neat PLA. These indicated that the addition of PEBA promoted the cold crystallization of PLA, which agreed well with the DMA results. Moreover, it can be seen that a further increase in the PEBA content had little effect on the position of the exotherm corresponding to the cold crystallization of PLA in the blends. In previous studies, similar phenomena were also reported in other immiscible PLA blends such as PLA/PCL and PLA/PBAT blends.[10,13] The enhancement of cold crystallization of the PLA in the blends may be induced by the interface between the phase-separated domains in the immiscible blends. The chains of the polymer segments near the interface will be different from that of the segments in the bulk at two aspects due to the presence of the interface in the multiphase systems. Firstly, an enrichment of chain ends, the shorter chains of the components and small third-molecule at the vicinity of the interface will improve the chain mobility of the polymer segments near the interface.[26,27] Recently, Roth and Torkelson pointed out that in the nanostructure or quasi-nanostructured immiscible polymer blend, an enhancement of chain mobility near interface might occur, causing a lower glass transition temperature.[28] Secondly, an enhancement of orientation ordering of polymeric coils may occur near the interface in the blends. Several researches had found that the enhanced segmental mobility near the free surface might result in an enhanced local ordering of the the near-surface chain.[26,29,30] Such localized alignment could act as a precursor to become crystallization. In poly(dimethylsiloxane) composites, Dollase and his coworkers suggested that the regions of non-random chain conformations on the intermediate length scales near the interface may play an important role in the early stages of crystallization, even if the orientation ordering of these regions does not match that of the lowest energy crystalline phase.[26] These regions may offer a different pathway for the crystallization by allowing the system to bypass its kinetic barriers that might delay the crystallization. In a semicrystalline polymer such as poly(ethylene terephthalate) (PET), an enhanced mobility at the surface in tandem with localized alignment was found to lead to a lower cold crystallization temperature and increased kinetics at the free surface.[31,32] These results had important implications for our understanding of the behaviors of polymer systems near interfaces. In immiscible blends, the influence of the interface between the phase-separated domains on the crystallization should be considered seriously.[10,26] Taking into account of the immiscibility for the PLA and PEBA in the blends, the sharp interface between the PLA and PEBA may play a favorable role in the cold crystallization of PLA in the blends.

As we have demonstrated above, the added PEBA elastomer improved the cold crystallization of PLA. This result is important both for the end-use and for the manufacturing of PLA, since in its amorphous form, its low glass transition temperature and the slow crystallization rate will limit its processability and thus its applications. Consequently, the non-isothermal crystallization behaviors of PLA and its PEBA blends were further exploited. The nonisothermal crystallization of the PLA/PEBA blends was studied by DSC at a cooling rate of 2 °C/min after melted at 190 °C for 5 min. Figure 6 depicts the DSC thermograms at a cooling stage. When the cooling rate was 2 °C/min, a clear exothermic peak from the crystallization of PLA was seen at ~98 °C for the neat PLA. Pure PEBA exhibited three exothermic peaks: one peak at about −11 °C, which was attributed to the crystallization of PTMO segments in PEBA and another two peaks at high temperature, which were associated with the crystallization of

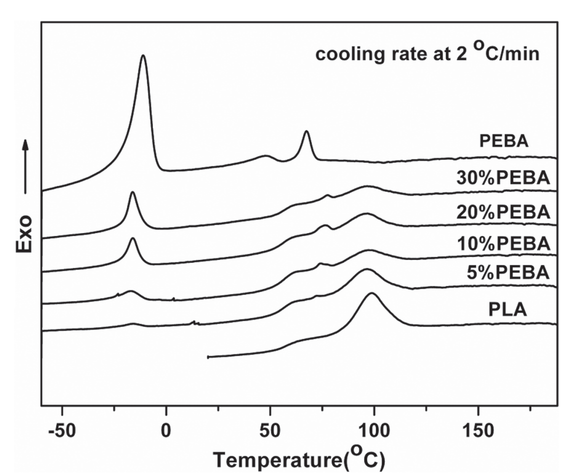

Fig. 6. The cooling DSC thermograms at a cooling rate of 2 °C/min for neat polymer and the blends after melted at 190 °C for 5 min.

ARTICLE

PA12 segments in PEBA.[25] As shown in Figure 6, the DSC cooling scan of the blends reveals all the three exothermic peaks corresponding to the crystallization of the component polymers. No obvious changes were observed for the crystallization temperature (T_c) of PTMO segments in the blends compared with neat PEBA. As for the crystallization of PLA in the blends, the T_c of PLA changed slightly from 98 °C for neat PLA to 96 °C for the blends, and then almost constant as the PEBA content increased. The interpretation of the crystallization of PA12 segments in PEBA was difficult because the small concentration of PA12 segment in the blends overlapped with the glass transition of PLA. However, it should be noted that the exothermic peaks of PA12 segments in the blends shifted a little to a higher temperature compared to pure PEBA. This result was because that the crystals of PLA might act as heterogeneous nucleating agents for the PA12. For a completely immiscible blend, crystallization is expected to occur separately for each of the melt phases. There was no significant change in the crystallization temperatures of the component polymers, indicating that the components crystallized separately from melting state in the blends due to the immiscibility between these two components.

3.3. Mechanical Properties of PLA/PEBA Blends

Figure 7 displays the typical tensile strain-stress curves of the samples. The average values of the tensile stress and elongation at break were provided in Figure 8. Neat PLA is a very rigid polymer and deforms in a brittle fashion, i.e., without obvious yield and low elongation at break: only ∼4%. However, the ductility of PLA was improved by the introduction of the PEBA elastomer. The blend underwent distinct yielding and considerable cold drawing after the yielding. This reflects a transition of the fracture behavior from brittle to ductile fracture. As shown in Figure 8, blending a small amount of PEBA was able to considerably improve the flexibility of PLA without reducing its tensile strength apparently. When 10 wt% PEBA was

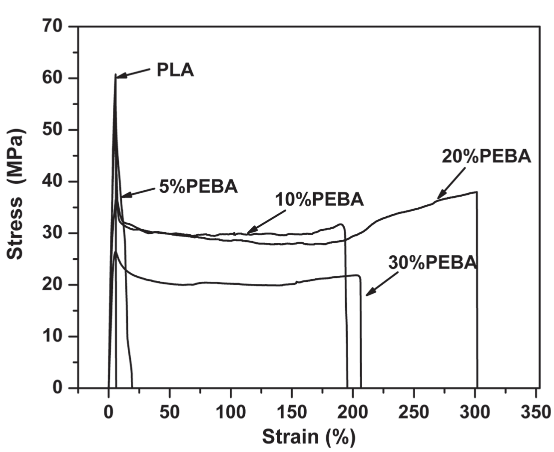

Fig. 7. Typical tensile stress–strain curves of PLA and PLA/PEBA blends.

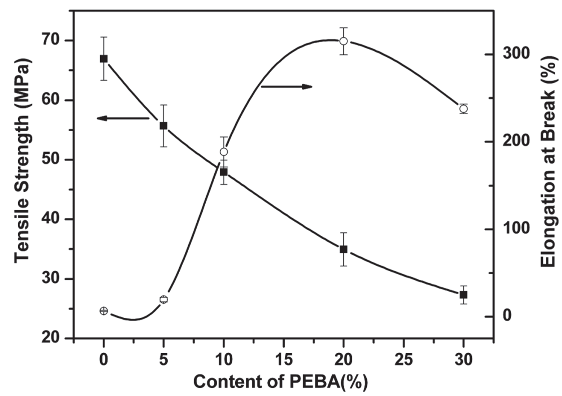

Fig. 8. Mechanical properties of PLA with various PEBA concentrations.

added, the elongation at break reached 188%, increased by above 40 times over pure PLA, while the yielding stress remained 48 MPa, slightly lower than neat PLA. The elongation at break increased initially from 4% for neat PLA to above 300% for the blend as the PEBA content was further increased to 20 wt%, and then decreased to 200% as the amount of PEBA in the blend increased to 30 wt%. The tensile strength and modulus of the PLA/PEBA blends decreased with increasing the PEBA content as expected due to the incorporation of a soft elastomeric phase to the PLA matrix.

The toughening mechanisms of PLA/PEBA blends were investigated through observing the morphology of different necking regions of the tensile-tested specimens by SEM. Figure 9 shows the SEM microstructures of the 10 wt% PEBA samples after the tensile testing. These SEM micrographs were taken at different locations of the necked down region, representing different deformation stages of the sample during the stretching. Debonding of the round PEBA particles from PLA matrix under tensile stress was clearly observed at the initial stage of the stretching, Figure 9(b). When the sample was subjected to the tensile stress, the domains of PEBA acted as the stress concentrators because of different elastic properties of the PEBA from that of the PLA. The stress concentration resulted in a high triaxial stress in the PEBA domains and the debonding occurred at the particle-martrix interface due to insufficient interfacial adhesion. The interfacial cavitation led to a relief of the triaxial stress state of the PLA matrix around the voids, thus creating a stress state beneficial for the initiation of multiple matrix shear yielding. As the yielding of the matrix happened, the stress was then applied to the PEBA domains. Then, with the debonding progresses, the orientation of both the matrix and the dispersed domains occurred, Figure 9(d). Similar toughening mechanism was also founded in other PLA blends, in which the improvement in toughness was achieved.[14, 21–23]

The increase in the elongation at break observed for the PLA/PEBA blends was concomitant with a significant increase in the impact strength of PLA as the concentration

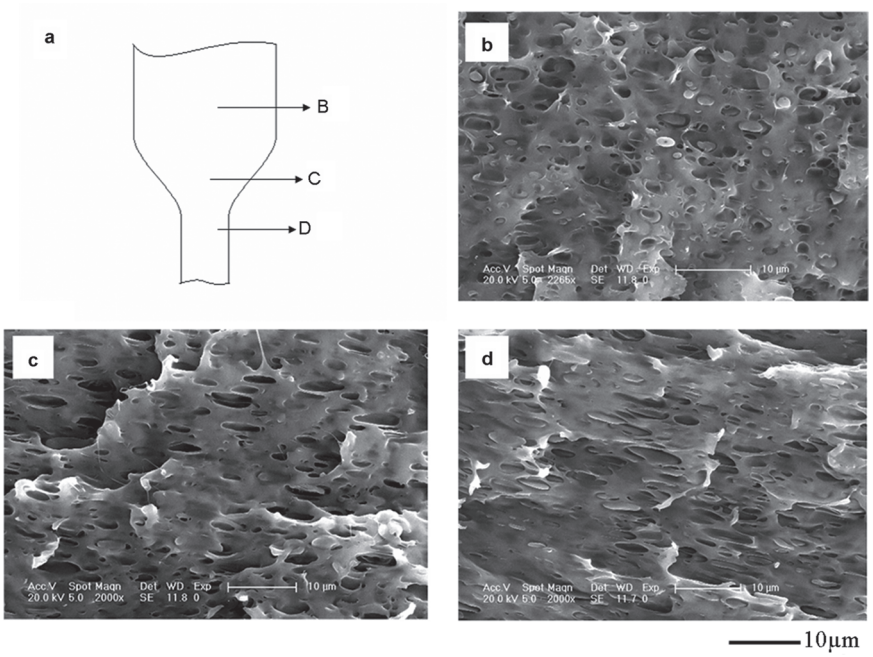

Fig. 9. SEM micrographs of the blend with 10 wt% PEBA at different locations of the necked down region during tensile testing.

of PEBA in the blends was increased. Figure 10 compares the impact strength of neat PLA with that of the blends at room temperature. All the blends clearly showed a higher impact strength than that of pure PLA. A rapid increase in impact strength was obtained at room temperature when more than 10 wt% PEBA was added. Significant improvement can be observed for blends with 20 wt% PEBA, about ten times bigger compared with neat PLA. The toughening effect of PLA/PEBA blends was studied further with the fracture surface of the impact specimen, Figure 11. Pure PLA showed a smooth and featureless fracture surface without much deformation, indicating a typical brittle fracture behavior. On the fracture surfaces of the blend with 5 wt% PEBA, multiple fracture surfaces replaced the single fracture lines. Some fibrils were discernible on the fracture surfaces. The toughening effect in this case remained moderate. The surface of the blend with 10 wt% PEBA became rougher and rougher with more and longer fibrils threads found, a clear evidence of the ductile fractures. With 20 wt% PEBA, significant plastic deformation of PLA matrix was evident, indicating a shear yielding. The PEBA particles could not be clearly defined from the matrix PLA. The corresponding amount of plastic deformation was high and effectively dissipated the fracture energy, which resulted in highly improved impact strengths at room temperature.

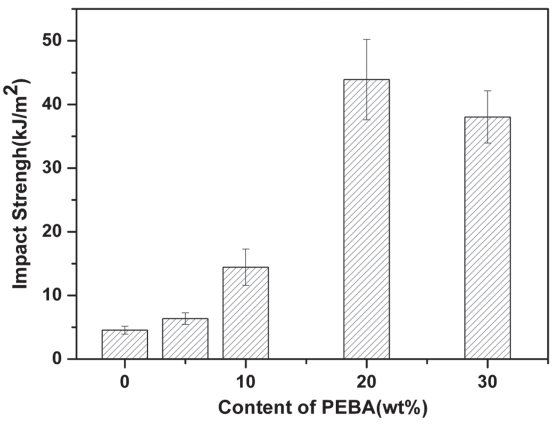

Fig. 10. Impact strength of PLA/PEBA blends as function of the weight fraction of PEBA.

3.4. Rheological Properties of PLA/PEBA Blends

Figure 12 shows the storage modulus (G'), loss modulus (G'') and complex viscosity (η^*) of neat polymers and PLA/PEBA blends as a function of frequency at 180 °C. There was a well developed dependence of the dynamic modulus on the PEBA contents at high frequencies: both the G' and G'' decreased with the increase of the PEBA content. However, it can be clearly seen from Figure 12(a) that for low frequencies, even at medium-frequency region, the G' of the blends for each composition is larger than those for the pure phases, and increases when the dispersed phase concentration increases. Generally, in immiscible blends, the enhancement of elasticity can be attributed to the relaxation process of the dispersed phase droplets when slightly sheared. When the dispersed phase concentration increased, the diameter of the dispersed phase increased and the relaxation process of the dispersed phase became longer, leading to an increase of the storage modulus.[33,34] Such non-terminal behavior has also been observed on other PLA based blend.[35,36] But it should be pointed out that in the PLA/PEBA blends, besides long relaxation

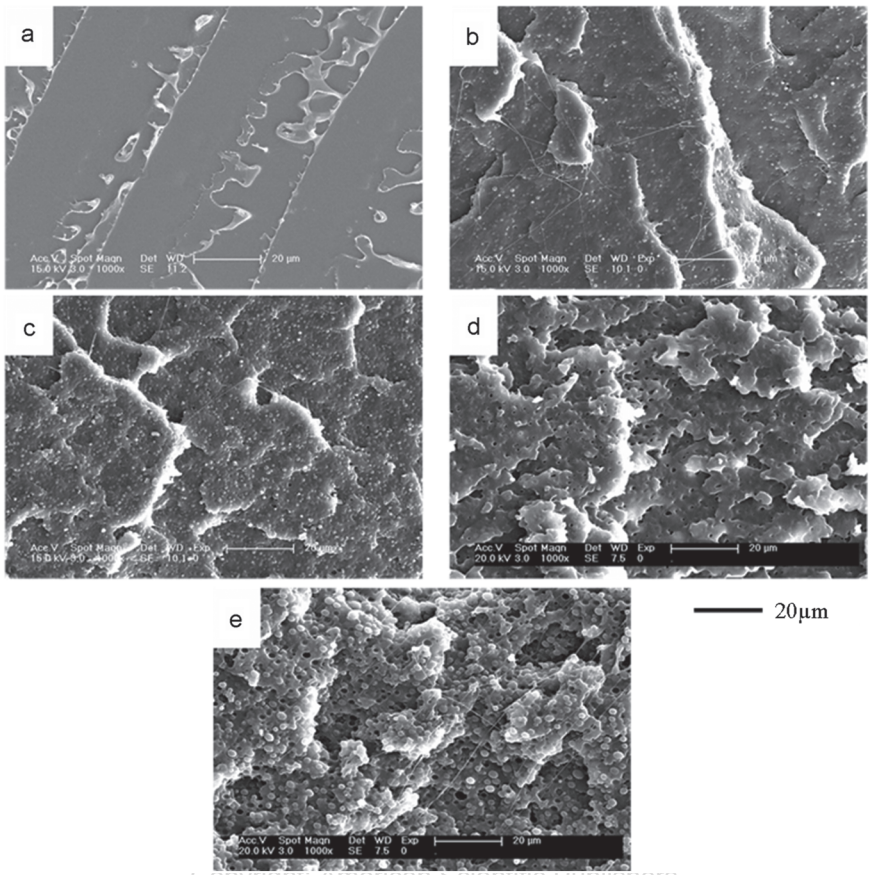

Fig. 11. SEM images of the impact-fracture surface of the PLA/PEBA blends with a PEBA weight percent of (a) 0, (b) 5, (c) 10, (d) 20, and (e) 30 wt%.

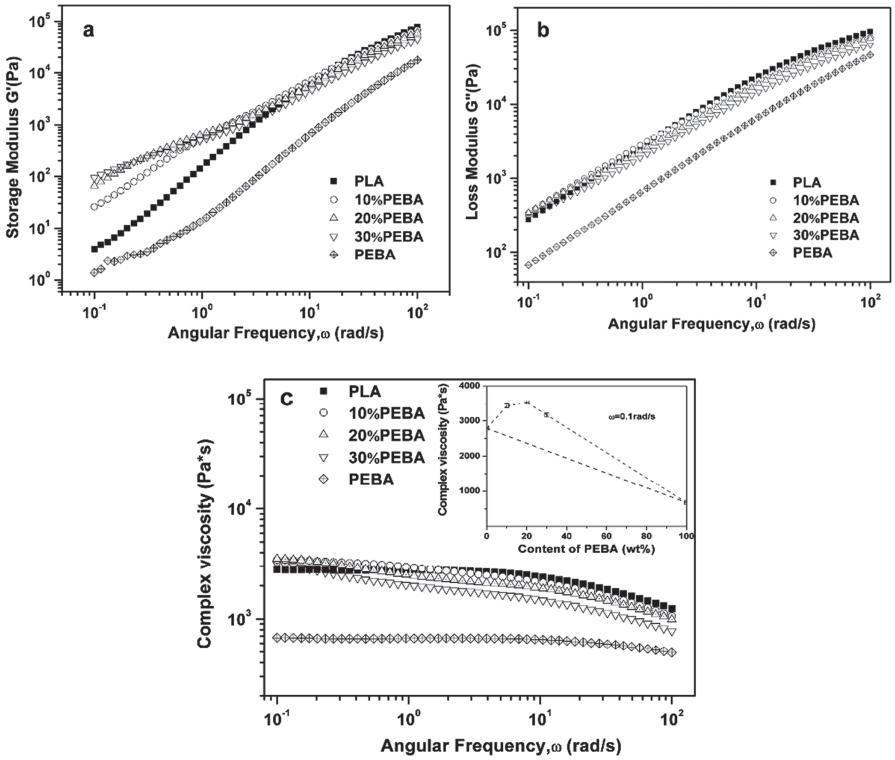

Fig. 12. (a) The storage modulus G′; (b) the loss modulus G′; and (c) complex viscosity of neat PLA, PEBA and the blends at 175 °C.

process of the dispersed phase, the interaction between the two phases will be an important reason for the enhanced G' at low frequency.

The viscoelastic response of the blends in low frequencies (low shear rates) can be used for evaluating of the interfacial interaction between phases. Because at low shear rates, the effect of flow induced molecular orientation on the viscosity and elasticity becomes much less.[37] As shown in Figure 12(c), at low frequency, the increase in the viscosity of the blends was also observed corresponding to the storage modulus. The experimental viscosity data were compared with the additive effect of the linear mixing rule,

$$\eta^*_{1,2} = \phi_1\eta^*_1 + \phi_2\eta^*_2 \quad (1)$$

where ϕ_1 and ϕ_2 are the weight ratio of the components 1 and 2, respectively, and η^*_1 and η^*_2 are the viscosities of the two components. According to this equation, Utracki divided viscosity-composition curve of the blends into three types: positive deviation blend (PDB); negative deviation blend (NDB); positive–negative deviation.[38] It was evident from the inset of Figure 11(c) that the experimental viscosity data of the blends exhibited a positive deviation at low frequency, which heavily suggested that there might be some interactions between PLA and PEBA under the experimental conditions. Though the blends were immiscible, there might be some interactions between these two components at the interface in the melt state. It was reported that the hydrogen bonding between the hard and soft segments of the PEBA was dissociated at higher temperature above the melting point of the hard segments.[39] It would be propitious to form an interaction between the N–H group in the hard segments of PEBA and the carbonyl groups of the PLA. The interaction between these two phases will reduce the possibility of the interlayer slip, and increase the formation of associative network, which may result in the yield stress.

4. CONCLUSIONS

Significant improvements in the flexibility and toughness were achieved in PLA by melt mixing it with a biocompatible thermoplastic poly(ether-*b*-amide) copolymer. DMA and DSC results indicated that the two components were immiscible. A clear, phase-separated morphology with PEBA dispersed in the PLA matrix was observed from the SEM results. Remarkably, by incorporating a small percentage of PEBA elastomer into PLA, the failure mode changed from the brittle fracture of the neat PLA to the ductile fracture of the blends as demonstrated by tensile test and the SEM micrographs of impact-fracture surface. An elongation at break of 300% was achieved for the blends with 20 wt% PEBA, as compared to 5% for the neat PLA, without significantly sacrificing the tensile strength of PLA matrix. A substantial increase in the notched Izod impact strength was also observed with increasing the content of PEBA in the blends. The cold crystallization of PLA was promoted by the presence of PEBA in the blends due to the interfacial function between the phases, while no obvious influence of PEBA on the crystallization of PLA from the melting state was observed. In addition, the viscosity and melt elasticity increased at low frequency with increasing the concentration of PEBA, indicating an interaction between PLA and PEBA in the melt state. This provides an opportunity to make high performance multifunctional polymer nanocomposites for different applications including electromagnetic interference shielding, water treatment, and various sensing.[40–51]

Acknowledgment: This work was supported by Zhejiang Provincial Natural Science Foundation of China under Grant No. LQ16E030008, the Quzhou Science and Technology Plan Project No. 2016Y002, and the Special Funds for the Construction of teaching staff in Quzhou University.

References and Notes

1. L. Yu, K. Dean, and L. Li, *Prog. Polym. Sci.* 36, 576 **(2006)**.
2. C. K. Williams and M. A. Hillmyer, *Polym. Rev.* 48, 1 **(2008)**.
3. L.-T. Lim, R. Auras, and M. Rubino, *Prog. Polym. Sci.* 33, 820 **(2008)**.
4. R. E. Drumright, P. R. Gruber, and D. E. Henton, *Adv. Mater.* 12, 1841 **(2000)**.
5. R. Auras, B. Harte, and S. Selke, *Macromol. Biosci.* 4, 835 **(2004)**.
6. K. S. Anderson, K. M. Schreck, and M. A. Hillmyer, *Polym. Rev.* 48, 85 **(2008)**.
7. J. Lunt, *Polym. Degrad. Stab.* 59, 145 **(1998)**.
8. H. Tsuji and Y. Ikada, *J. Appl. Polym. Sci.* 60, 2367 **(1996)**.
9. M. E. Broz1, D. L. VanderHart, and N. R. Washburn, *Biomaterials* 24, 4181 **(2003)**.
10. R. Dell'Erba, G. Groeninckx, G. Maglio, M. Malinconico, and A. Migliozzi, *Polymer* 42, 7831 **(2001)**.
11. I. Noda, M. M. Satkowski, A. E. Dowrey, and C. Marcott, *Macromol. Biosci.* 4, 269 **(2004)**.
12. M. Shibata, Y. Inoue, and M. Miyoshi, *Polymer* 47, 3557 **(2006)**.
13. L. Jiang, M. P. Wolcott, and J. W. Zhang, *Biomacromolecules* 7, 199 **(2006)**.
14. J. M. Lu, Z. B. Qiu, and W. T. Yang, *Polymer* 48, 4196 **(2007)**.
15. T. Y. Liu, W. C. Lin, M. C.Yang, and S. Y. Chen, *Polymer* 46, 12586 **(2005)**.
16. O. Martin and L. Avérous, *Polymer* 42, 6209 **(2001)**.
17. K. S. Anderson, S. H. Lim, and M. A. Hillmyer, *J. Appl. Polym. Sci.* 89, 3757 **(2003)**.
18. Y. Parulekar and A. K. Mohanty, *Green Chem.* 8, 206 **(2006)**.
19. D. Grijpma, D. Van Hofslot, A. Supér, A. Nijenhuis, and A. Pennings, *Polym. Eng. Sci.* 34, 1674 **(1994)**.
20. T. N. Li, L. S. Turng, S. Q. Gong, and K. Erlacher, *Polym. Eng. Sci.* 46, 1419 **(2006)**.
21. Y. J. Li and H. Shimizu, *Macromol. Biosci.* 7, 921 **(2007)**.
22. R. Bhardwaj and A. K. Mohanty, *Biomacromolecules* 8, 2476 **(2007)**.
23. Y. Lin, K. Y. Zhang, Z. M. Dong, L. S. Dong, and Y. Li, *Macromolecules* 40, 6257 **(2007)**.
24. M. R. Barzegari, N. Hossieny, D. Jahani, and C. B. Park, *Polymer* 114, 15 **(2017)**.
25. J. P. Sheth, J. N. Xu, and G. L. Wilkes, *Polymer* 44, 743 **(2003)**.
26. T. Dollase, M. Wilhelm, H. W. Spiess, Y. Yagen, R. Yerushalmi-Rozen, and M. Gottlieb, *Interface Science* 11, 199 **(2003)**.
27. A. M. Mayes, *Macromolecules* 27, 3114 **(1994)**.

ARTICLE

28. C. B. Roth, K. L. McNerny, W. Jager, and J. Torkelson, *Macromolecules* 40, 2568 **(2007)**.
29. B. J. Factor, T. P. Russell, and M. F. Toney, *Phys. Rev. Lett.* 66, 1181 **(1991)**.
30. M. F. Toney and T. P. Russell, *Nature* 374, 709 **(1995)**.
31. P. C. Jukes, A. Das, M. Durell, D. Trolley, A. M. Higgins, M. J. Geoghegan, E. Macdonald, R. A. L. Jones, S. Brown, and P. Thompson, *Macromolecules* 38, 2315 **(2005)**.
32. D. H. Lee, K. H. Park, Y. H. Kim, and H. S. Lee, *Macromolecules* 40, 6277 **(2007)**.
33. M. Bousmina, *Rheol. Acta* 3, 73 **(1999)**.
34. P. S. Calvão, Y. Marcio, and N. R. Demarquette, *Polymer* 46, 2610 **(2005)**.
35. D. F. Wu, Y. S. Zhang, M. Zhang, and W. D. Zhou, *Eur. Polym. J.* 44, 2171 **(2008)**.
36. S. Y. Gu, K. Zhang, J. Ren, and H. Zhan, *Carbohydr. Polym.* 74, 79 **(2008)**.
37. M. Faker, M. K. Razavi, M. Ghaffari, and S. A. Seyyedi, *Eur. Polym. J.* 44, 1834 **(2008)**.
38. L. A. Utracki and M. R. Kanial, *Polym. Eng. Sci.* 22, 96 **(1982)**.
39. I. K. Yang and P. H. Tsai, *J. Polym. Sci. Part B: Polym. Phys.* 43, 2557 **(2005)**.
40. J. Guo, H. Song, H. Liu, C. Luo, Y. Ren, T. Ding, M. A. Khan, D. P. Young, X. Liu, X. Zhang, J. Kong, and Z. Guo, *J. Mater. Chem. C* 5, 5334 **(2017)**.
41. Y. Ma, J. Mai, L. Wu, G. Fang, and Z. Guo, *Polymer* 114, 113 **(2017)**.
42. K. Zhang, H. Yu, Y. Shi, Y. Chen, J. Zeng, J. Guo, B. Wang, Z. Guo, and M. Wang, *J. Mater. Chem. C* 5, 2807 **(2017)**.
43. H. Liu, M. Dong, W. Huang, J. Gao, K. Dai, J. Guo, G. Zheng, C. Liu, C. Shen, and Z. Guo, *J. Mater. Chem. C* 5, 73 **(2017)**.
44. C. Alippi, *CAAI Trans. Intelligence Technol.* 1, 1 **(2016)**.
45. H. Jin, Q. Chen, Z. Chen, Y. Hu, and J. Zhang, *CAAI Trans. Intelligence Technol.* 1, 104 **(2016)**.
46. H. Liu, J. Gao, W. Huang, K. Dai, G. Zheng, C. Liu, C. Shen, X. Yan, J. Guo, and Z. Guo, *Nanoscale* 8, 12977 **(2016)**.
47. X. Zhang, H. Gao, M. Guo, G. Li, Y. Liu, and D. Li, *CAAI Trans. Intelligence Technol.* 1, 4 **(2016)**.
48. H. Gu, J. Guo, H. Wei, S. Guo, J. Liu, Y. Huang, M. A. Khan, X. Wang, D. P. Young, S. Wei, and Z. Guo, *Adv. Mater.* 27, 6277 **(2015)**.
49. C. Hu, Z. Li, J. Gao, K. Dai, G. Zheng, C. Liu, C. Shen, H. Song, and Z. Guo, *J. Mater. Chem. C* 5, 2318 **(2017)**.
50. Z. Sun, L. Zhang, F. Dang, Y. Liu, Z. Fei, Q. Shao, H. Lin, J. Guo, L. Xiang, N. Yerra, and Z. Guo, *CrystEngComm.* **(2017)**, in press, DOI: 10.1039/C7CE00279C.
51. S. Padhy and S. Panda, *CAAI Trans. Intelligence Technol.* 2, 12 **(2017)**.